3D Geometric Primitive Alignment Revisited

Trung-Thien Tran, Van-Toan Cao and Denis Laurendeau
Computer Vision and Systems Laboratory, Laval University, 1065, avenue de la Medecine, Quebec, G1V 0A6, Canada

Keywords: Plane, Cylinder, Sphere, Primitive-based Alignment, Rigid Registration, Coarse Registration.

Abstract: Rigid registration is an important step in 3D scanning and modeling of manufactured objects that are generally composed of a combination of basic geometric primitives such as planes, spheres, cylinders, etc. In this paper, an efficient and robust method is proposed to align two basic geometric primitives. The transformation between two primitives is found by minimizing the parameter error between primitive correspondences. The approach applies an interior-point method and a new objective function to achieve good results. Compared to previous primitive-based alignment approach proposed by Rabbani et al. (Rabbani et al., 2007), the presented approach achieves better results in terms of convergence and accuracy. Finally, the proposed method is used in various applications such as data completion and primitive-based registration for quality control and inspection.

1 INTRODUCTION

3D sensors are being used more and more widely in several applications, especially in industrial manufacturing. Since the field of view of these sensors is limited, it is necessary to scan an object from different viewpoints in order to cover its complete surface. These local scans are then used in the modeling and reconstruction process. Among common problems, a registration step is inevitable to transform all of the scans into a common coordinate reference frame. Registration is also referred to as alignment or matching, so these terms are used interchangeably throughout the paper.

The 3D registration problem can be classified in several ways. On one hand, according to the rigidity of the objects, registration is categorized as rigid and non-rigid as summarized in (Tam et al., 2013). On the other hand, following the quality of the result, registration methods can also be classified as coarse registration (Planitz et al., 2005; Díez et al., 2015) and fine registration (Besl and McKay, 1992; Rusinkiewicz and Levoy, 2001; Salvi et al., 2007). In this paper, we investigate the problem of *coarse registration* in which the parts are aligned roughly with each other. From now on, the word registration will refer to the coarse registration problem.

Currently, registration methods often address the problem of aligning meshes or point clouds having similar densities of data points. 3D descriptors (Díez et al., 2015) are proposed and keypoints (Tombari et al., 2013) are extracted from 3D data for correspondence and shape matching. However, most existing descriptors and keypoints fail to register two scans of man-made objects, because the main challenge is to propose a descriptor that is able to deal with symmetrical and similar geometries from the primitive surfaces.

Some research has been conducted to align datasets using primitives as descriptors. The primitives could be linear and circular features as in (Stamos et al., 2008) or planes in (Bosché, 2012). Linear features (Chao and Stamos, 2005) between two planes and circular features (Stamos et al., 2008) from 2D and range images of buildings and urban scenes are used. Bosche's approach (Bosché, 2012) use planes that are extracted at a single point selected by the user. Iterative Closest Point (ICP) is then used to compute the transformation using three pairs of plane correspondences. Rabbani et al. (Rabbani et al., 2007) have also used geometric primitives such as planes, cylinders and spheres for registration and modeling. The method minimizes the sum of squares of the differences of parameters by using the Levenberg-Marquardt optimization (LM) (Marquardt, 1963). The proposed approach exploits this idea and brings many improvements in terms of convergence and accuracy.

The contributions of the paper are summarized as follows.

Tran, T-T., Cao, V-T. and Laurendeau, D.
3D Geometric Primitive Alignment Revisited.
DOI: 10.5220/0005715800890096
In *Proceedings of the 11th Joint Conference on Computer Vision, Imaging and Computer Graphics Theory and Applications (VISIGRAPP 2016) - Volume 1: GRAPP*, pages 91-98
ISBN: 978-989-758-175-5

- A robust approach is proposed to align geometric primitives. Each type of primitive (plane, sphere, cylinder) is described in detail in Sec. 2.3.
- A new minimization technique is exploited to achieve better results than other techniques with respect to convergence and error of descriptive parameters.
- The proposed method is used in primitive-based alignment and quality control applications, which registers two scans to create an error map or complete model of the object of interest.

2 PRIMITIVE ALIGNMENT

2.1 Quaternion Representation

Rigid registration consists of finding a unique transformation $\mathbf{T} : R^3 \mapsto R^3$, which brings two datasets as close as possible. This transformation is expressed as a 3x3 rotation matrix $\mathbf{R}$ and a translation vector $\mathbf{t} = \{t_x, t_y, t_z\}$. Horn (Horn, 1987) has proposed a closed-form solution for determining a rotation matrix using a quaternion representation. With a given quaternion $\mathbf{q} = \{q_0, q_1, q_2, q_3\}$, the rotation matrix $\mathbf{R}$ is computed as

$$\mathbf{R} = \begin{pmatrix} 2q_0^2+2q_1^2-1 & 2(q_1q_2-q_0q_3) & 2(q_1q_3+q_0q_2) \\ 2(q_1q_2+q_0q_3) & 2q_0^2+2q_2^2-1 & 2(q_2q_3-q_0q_1) \\ 2(q_1q_3-q_0q_2) & 2(q_2q_3+q_0q_1) & 2q_0^2+2q_3^2-1 \end{pmatrix}$$

with the constraint $\|\mathbf{q}\| = \sqrt{q_0^2+q_1^2+q_2^2+q_3^2} = 1$ which guarantees a rotation operator in R^3 having only three degrees of freedom.

2.2 Rabbani's Approach and Associated Drawbacks

Rabbani et al. (Rabbani et al., 2007) have proposed an approach that combines registration and modeling in one framework. At the registration step, quaternion and geometric primitives are used to align two scans called S_1 and S_2, respectively. The transformation $\mathbf{T}$ is calculated using a least-squares algorithm in the parameter space of the primitives. In other words, this step minimizes the sum of the square of errors of primitive parameters as follows:

$$\min_{\{\mathbf{R}(\mathbf{q}),t\}} \sum_{i}^{|\mathbf{C}|} \sum_{j}^{\mathbf{M_i}} \Delta_{u_{ij}}^2 \tag{1}$$

where $\Delta_{u_{ij}} = u_{ij}^{S_1} - \mathbf{T}(u_{ij}^{S_2})$ and u_{ij} is the j-th parameter of the i-th correspondence that has $|M_i|$ criteria of parameter convergence. $\mathbf{C}$ is the set of correspondences. For example, when the first correspondence pair is plane-plane, $|M_1|$ is equal to 2 since there is a criterion for the error on the normal vector and another criterion for the error on the distance to the origin. The mathematical equations for each single primitive are expressed later in Sec. 2.3.

The Levenberg-Marquardt optimization (Marquardt, 1963) is used to solve the non-linear least-squares problem in Eq. 1. Partial derivatives of Δ w.r.t of rotation $\mathbf{R}$ and translation $\mathbf{t}$ are required and computed as

$$\left\{ \frac{\partial\Delta}{\partial q_0}, \frac{\partial\Delta}{\partial q_1}, \frac{\partial\Delta}{\partial q_2}, \frac{\partial\Delta}{\partial q_3}, \frac{\partial\Delta}{\partial t_x}, \frac{\partial\Delta}{\partial t_y}, \frac{\partial\Delta}{\partial t_z} \right\}$$

These derivatives are used to compute the Jacobian matrix $\mathbf{J}$ and update the transformation parameter $\Gamma = \{\mathbf{q}, \mathbf{t}\}$ as follows:

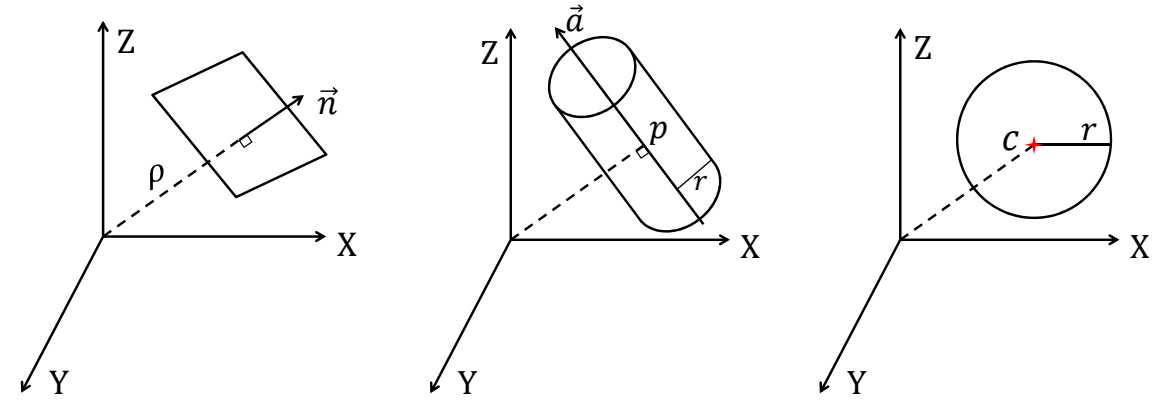

(a) Plane represented by normal vector $\vec{n}$ and the distance to the origin ρ.

(b) Cylinder described by axis vector $\vec{a}$, radius r and a closest point to the origin in axis $\mathbf{p}$.

(c) Sphere represented by center $\mathbf{c}$ and radius r

Figure 1: Representative parameter of primitives: plane, cylinder and sphere.

$$\Gamma = \{\mathbf{q}, \mathbf{t}\} = \{q_0, q_1, q_2, q_3, t_x, t_y, t_z\} \quad (2)$$

$$\Gamma_{t+1} = \Gamma_t - (\mathbf{J}^T\mathbf{J} + \lambda\mathbf{I})^{-1}\mathbf{J}\Delta \quad (3)$$

$$\mathbf{J} = \frac{\partial \Delta}{\partial \Gamma}; \quad (4)$$

where t is the iteration step, and $\mathbf{J}$ is the Jacobian matrix. Observing Eq.3, the Levenberg-Marquardt optimization consists of Gauss-Newton and Steepest descent methods by using a non-negative scalar λ, which is called the Levenberg-Marquardt parameter. The selection of λ and its impact on convergence are discussed in (Press et al., 2007). Generally, Levenberg-Marquardt optimization achieves better convergence compared to Gauss-Newton and Steepest descent methods taken separately.

Rabbani's approach faces many problems that have an impact on the convergence of the result.

- First, the LM optimization generally provides a solution to an unconstrained problem. Therefore, the method does not guarantee that the solution provides a unit quaternion $\|\mathbf{q}\| = 1$ for each iteration of the optimization loop. This leads to poor results for the rotation matrix $\mathbf{R}$. This behavior has been tested in the experiments reported in Sec. 3. The method proposed in this paper uses an interior point technique with constraints to guarantee that condition ($\|\mathbf{q}\| = 1$) is satisfied.
- Second, the objective function for cylinders lacks a robust criterion for alignment, which has an adverse effect on convergence. The proposed approach complements the objective function with a new criterion that guarantees good convergence (Eq. 8).

2.3 Proposed Approach for Primitive Alignment

In this section, the detailed framework for registering two primitives is presented. These primitives can be planes, cylinders and spheres. We assume the correspondence pairs $\mathbf{C} = \{\mathbf{S_1}, \mathbf{S_2}\}$ between primitives are already determined. The transformation $\mathbf{T} = \{\mathbf{R}, \mathbf{t}\}$ is computed by minimizing the following cost function.

$$\min_{\{\mathbf{R}(\mathbf{q}),t\}} \sum_{i}^{|\mathbf{C}|} \sum_{j}^{\mathbf{M_i}} \Delta_{u_{ij}}^2$$
$$\text{subject to:} \|\mathbf{q}\| = \sqrt{q_0^2 + q_1^2 + q_2^2 + q_3^2} = 1 \quad (5)$$

where the error is defined as $\Delta_{u_{ij}} = u_{ij}^{S_1} - \mathbf{T}(u_{ij}^{S_2})$.

To solve the non-linear least-squares problem in Eq. 5, the interior-point method (Forsgren et al., 2002) is used. The interior point method guarantees that the constraint $\|\mathbf{q}\| = 1$ is always satisfied at each iteration of the optimization loop. The mathematical equations for aligning each type of primitive are described in the following.

2.3.1 Plane

Planes are geometric primitives frequently found on manufactured objects. A plane is represented by a normal vector $\vec{\mathbf{n}}$ and a distance from the closest point to the origin ρ, as shown in Fig. 1(a). Assume that there are two planes with parameters $\{\vec{\mathbf{n}}_1, \rho_1\}$ and $\{\vec{\mathbf{n}}_2, \rho_2\}$, respectively.

To align plane 2 to plane 1, the error on the normal vector and the error on the distance to the origin are minimized as follows:

$$\vec{\mathbf{n}}_\delta = \vec{\mathbf{n}}_1 - \mathbf{R}\vec{\mathbf{n}}_2 \quad (6)$$

$$\rho_\delta = \rho_2 - \rho_1 + (\mathbf{R}\vec{\mathbf{n}}_2)^T\mathbf{t} \quad (7)$$

Eq. 6-7 are fed to Eq. 5 for the minimization step.

2.3.2 Cylinder

A cylinder is described by three parameters: its axis vector $\overrightarrow{d}$, its radius r and a closest point to the origin on the cylinder axis $\mathbf{p}$, as shown in Fig. 1(b). To bring a cylinder $C_2 = \{\overrightarrow{\mathbf{a}}_2; \mathbf{p}_2; r\}$ as close as possible to a cylinder $C_1 = \{\overrightarrow{\mathbf{a}}_1; \mathbf{p}_1; r\}$, two points $\mathbf{p}_1$ and $\mathbf{p}_2$ and two vectors $\overrightarrow{\mathbf{a}}_1$ and $\overrightarrow{\mathbf{a}}_2$ need to coincide.

$$\vec{\mathbf{a}}_\delta = \vec{\mathbf{a}}_1 - \mathbf{R}\vec{\mathbf{a}}_2 \quad (8)$$

$$\vec{\mathbf{p}}_\delta = \mathbf{R}\vec{\mathbf{p}}_2 + \mathbf{t} - (\vec{\mathbf{a}}_\mathbf{R} * \mathbf{t}^T)\vec{\mathbf{a}}_\mathbf{R} - \vec{\mathbf{p}}_1 \quad (9)$$

where $\vec{\mathbf{a}}_\mathbf{R} = \mathbf{R}\vec{\mathbf{a}}_2$

Eq. 8-9 are fed to Eq. 5 for the minimization step.

2.3.3 Sphere

A sphere is simply represented by its center $\mathbf{c}$ and radius r, as shown in Fig. 1(c). To align a sphere 2 $\{\mathbf{c}_2, r\}$ to sphere 1 $\{\mathbf{c}_1, r\}$, the two centers need to coincide ($\mathbf{c}_\delta = 0$).

$$\mathbf{c}_\delta = \mathbf{R}\mathbf{c}_2 + \mathbf{t} - \mathbf{c}_1 \quad (10)$$

Eq. 10 is fed to Eq. 5 for the minimization step.

The framework is applied to align a set of several multiple primitives simultaneously. The objective functions of each primitive pair are combined and minimized in Eq. 5. When the minimization ends, the transformation between the datasets is available.

3 RESULTS AND DISCUSSION

In this section, the results of the proposed approach are compared to the ones reported by Rabbani's in

(Rabbani et al., 2007). Both methods use geometric primitives for alignment. The sets of primitives $\Psi_1 = \{\mathbf{P}_1, \mathbf{C}_1, \mathbf{S}_1\}$ and their parameters are known a priori. Dataset Ψ_1 is transformed by 100 sets of transformation $\mathbf{T}$ randomly generated to create new sets of primitives $\Psi_2 = \{\mathbf{P}_2, \mathbf{C}_2, \mathbf{S}_2\}$. Then four experiments are conducted.

- Experiment 1: The transformation $\mathbf{T}'$ needed to transform plane $\mathbf{P}_2$ to plane $\mathbf{P}_1$ is estimated. The convergence is evaluated by

$$\cos(\angle(\mathbf{T}'(\mathbf{n}_{P_2}), \mathbf{n}_{P_1})) == 1 \quad (11)$$

- Experiment 2: The transformation $\mathbf{T}'$ needed to align cylinder $\mathbf{C}_2$ to cylinder $\mathbf{C}_1$ is estimated. The convergence is evaluated by

$$\cos(\angle(\mathbf{T}'(\mathbf{a}_{C_2}), \mathbf{a}_{C_1})) == 1 \quad (12)$$

- Experiment 3: The transformation $\mathbf{T}'$ to align a sphere $\mathbf{S}_2$ to sphere $\mathbf{S}_1$ is also computed. The convergence is then evaluated by

$$\|\mathbf{c}_{S_1} - \mathbf{T}'(\mathbf{c}_{S_2})\|_2 == 0 \quad (13)$$

- Experiment 4: All types of primitives are combined simultaneously into the framework. The convergence is reached if Eq. 11-13 are satisfied simultaneously.

The proposed framework is implemented on MATLAB on a 3.2 GHz Intel Core i7 platform. In the implementation of primitive alignment, Rabbani et al. (Rabbani et al., 2007) use Levenberg-Maquardt non-linear optimization which is implemented in the ***lsqnonlin*** function in MATLAB. The proposed framework rather uses the ***fmincon*** function which is implemented for the interior-point method. The percentage of success and the error on the parameters are investigated for both methods.

3.1 Success Rate of the Proposed Method

With 100 randomly generated sets of transformations, four alignment experiments are carried out and the conditions in Eq. 11-13 are checked sequentially or simultaneously. Fig. 2 illustrates the success rate of both methods LM_Rabbani and IP_OUR in the four experiments.

Rabbani's method is able to align planar and sphere primitives, but fails with cylinder primitives, as shown in Fig. 2. Therefore, in general, Rabbani's method cannot align a set of multiple primitives. The approach proposed in this paper achieves high success rates for all cases ($> 90\%$).

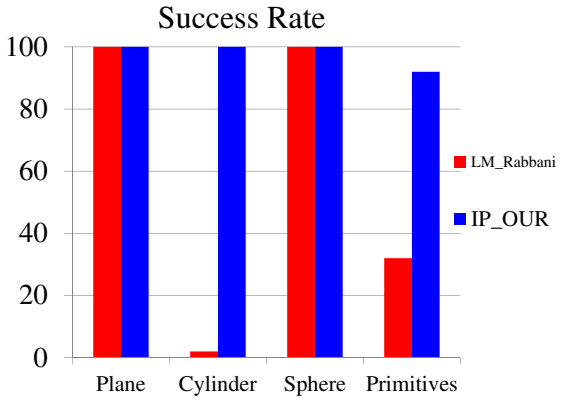

Figure 2: Success rate for Rabbani's method (LM_Rabbani) and the proposed method (IP_OUR).

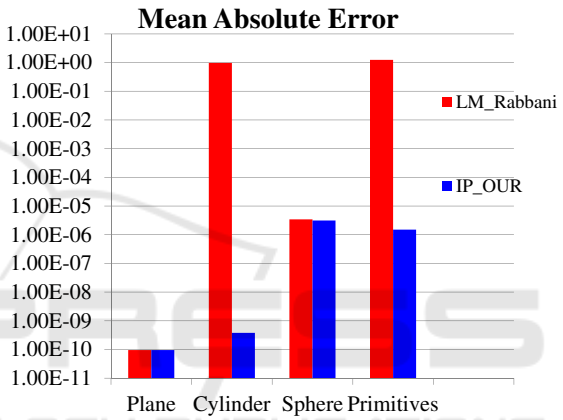

Figure 3: Logarithmic graph of mean absolute errors for Rabbani's method (LM_Rabbani) and our method (IP_OUR).

3.2 Errors on Primitive Parameters

The mean absolute error (MAE) values in Eq. 11-13 are computed for each of the 100 random sets of transformation.

- Experiment 1: The error on the plane normal after transformation is computed as follows:

$$\text{MAE}_P = \frac{1}{100}\sum_{i=1}^{100}\left(1 - |\cos(\angle(\mathbf{T_i}'(\mathbf{n}_{P_2}), \mathbf{n}_{P_1}))|\right) \quad (14)$$

- Experiment 2: The error on axis directions of the cylinders after transformation is computed as:

$$\text{MAE}_C = \frac{1}{100}\sum_{i=1}^{100}\left(1 - |\cos(\angle(\mathbf{T_i}'(\mathbf{a}_{C_2}), \mathbf{a}_{C_1}))|\right) \quad (15)$$

- Experiment 3: The error of the sphere centers af-

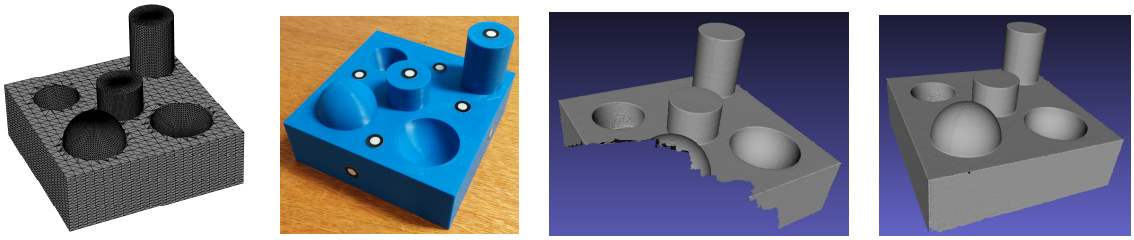

(a) CAD model designed with 3DS Max. (b) The plastic object printed with a Stratasys Dimension 1200es printer. (c) A partial scan of the plastic model scanned with the GO!SCAN 3D sensor. (d) Complete scan of the plastic model.

Figure 4: The plastic object is printed and scanned to create partial and complete scan datasets.

ter transformation is computed:

$$\mathrm{MAE}_S = \frac{1}{100}\sum_{i=1}^{100}\left(\|\mathbf{c}_{S_1} - \mathbf{T_i}'(\mathbf{c}_{S_2})\|_2\right) \quad (16)$$

- Experiment 4: The error on combined primitives taken altogether is computed as:

$$\mathrm{MAE}_\Sigma = \mathrm{MAE}_P + \mathrm{MAE}_C + \mathrm{MAE}_S \quad (17)$$

A logarithm plot of the MAE for the four experiments is shown in Fig. 3. The proposed method clearly outperforms Rabbani's method in aligning primitives.

From the results of the experiments, it is concluded that the proposed method, which combines a new optimization technique and a new objective function, solves the problem of primitive-based alignment with better results with respect to convergence and error of descriptive parameters.

One more experiment has been conducted to show the performance of the proposed method. The estimated transformation $\mathbf{T}'$ in the 4th experiment is compared to the ground-truth transformation $\mathbf{T}$ as follows:

- The error of rotation matrix is defined as:

$$\mathrm{E}_\mathbf{R} = \frac{1}{100}\sum_{i=1}^{100}\|\mathbf{R} - \mathbf{R}'\|_2 = 6.85e^{-7} \quad (18)$$

- Translation vector is commutative, so the error of translation is computed by:

$$\mathrm{E}_\mathbf{t} = \frac{1}{100}\sum_{i=1}^{100}\left|\|\mathbf{t}\| - \|\mathbf{t}'\|\right| = 2.68e^{-6} \quad (19)$$

The values of $\mathrm{E}_\mathbf{R}$ and $\mathrm{E}_\mathbf{t}$ prove that the proposed method estimates the transformation between datasets accurately.

3.3 Application of the Proposed Approach on Real 3D Scans

The first application is to register the scanned data of a printed 3D object with its CAD model. The object is printed with a Stratasys Dimension 1200es printer (Fig. 4(b)) and scanned by the Creaform GO!SCAN 3D scanner. Markers are used by the scanner for self positioning. This part-to-CAD problem is frequently used in quality control and inspection applications. The proposed framework for primitive alignment is applied as follows in this case. First, primitives from the point cloud are extracted using the method in (Tran et al., 2015b), and primitives from the CAD model are extracted by the approached proposed in (Attene et al., 2006). The correspondence pairs of primitives are defined manually. After being aligned, the distances between points and the CAD model are computed to generate an error map, as shown in Fig. 5. In this experiment, the scanned object's pose is close to the one of the CAD model.

Observing the results in Fig. 5, it is observed that our method outperforms Rabbani's approach in terms of alignment errors (Fig. 5(b)-5(c)). On the histograms of the error maps, the error of our method is smaller than the one of Rabbani's approach. The reason is that Rabbani's approach does not guarantee the condition ($\|\mathbf{q}\| = 1$) when LM optimization updates the parameters in the minimization process. Moreover, the lack of objective function for cylinders has a significant influence on convergence. The proposed method solves these two problems and achieves better alignment result.

A more challenging experiment has been conducted in which the pose of the scanned object is in the opposite direction of the one of the CAD model (Fig 6). Rabbani's method fails to align the datasets while the proposed method achieves a good alignment result with an error map similar to the one in Fig 5(c).

The second application of the proposed approach is data completion. The complete model of an object is often built from multiple partial scans. Separate scans are needed and must be expressed in a common coordinate frame using registration. In this section, the proposed method is used to register two real scans. In Fig. 7, two scans of the object in Fig. 7(a) are

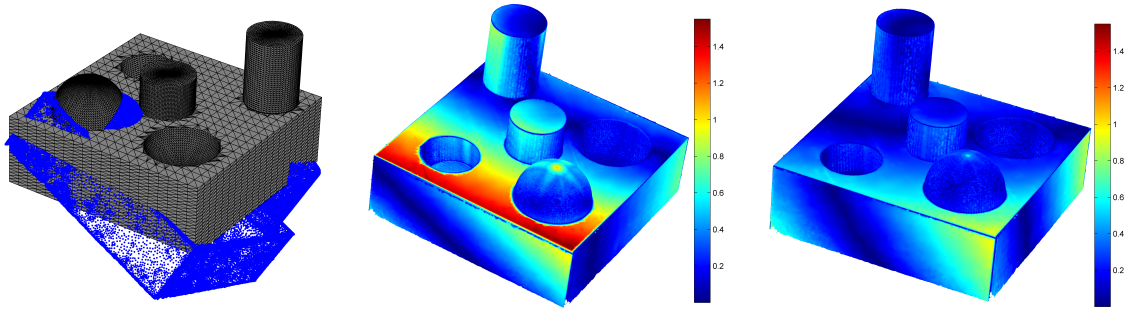

(a) Scanned data and CAD model. (b) Error map of the result for Rabbani's approach. (c) Error map of the result for the proposed approach.

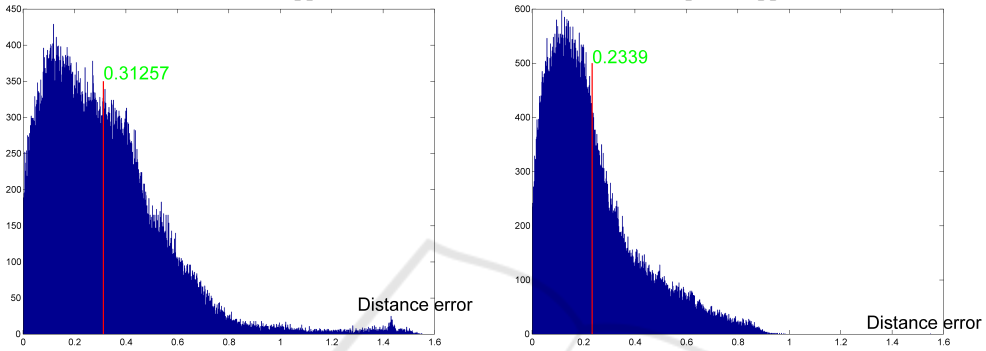

(d) Histogram of the error map created from Rabbani's approach, largest value (1.55) mean error value (0.31).

(e) Histogram of the error map generated from our proposed method, largest value (0.98) and mean error value (0.23).

Figure 5: Alignment of scanned data with its CAD model. Error maps of both methods are created and analyzed. The distance error of our method is smaller than the one of Rabbani's approach.

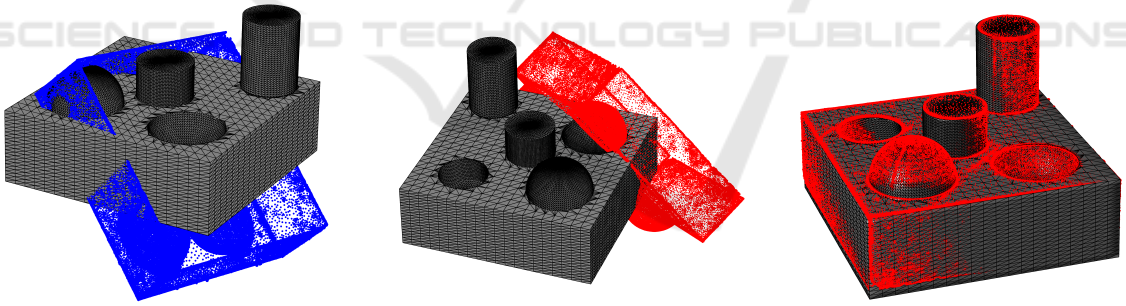

(a) (b) (c)

Figure 6: Comparison between two methods in the case where the pose of the scanned object is in the opposite direction of that of the CAD model. (a) Datasets with opposite pose between the scan and its CAD model. (b) Rabbani's method fails to align the datasets. (c) Good alignment result is still achieved by the proposed method.

shown. First, planar, cylindrical and spherical primitives are extracted from the scans using the method reported in (Tran et al., 2015a; Tran et al., 2016; Tran et al., 2015b). These primitives are then fed to the alignment approach presented in Sec. 2.3 to build a complete model of the object. The resulting model is shown in Fig. 7(b). The same strategy is used for the planes on two point clouds of the church in Fig. 7(c) with the resulting model in Fig. 7(d) after alignment using planar primitives.

Although primitive correspondences are selected manually by the user, this operation is not difficult even for a novice. In addition, this operation is easier than choosing the points used in manual ICP (Besl and McKay, 1992) and the other approach proposed in Bosche et al. (Bosché, 2012).

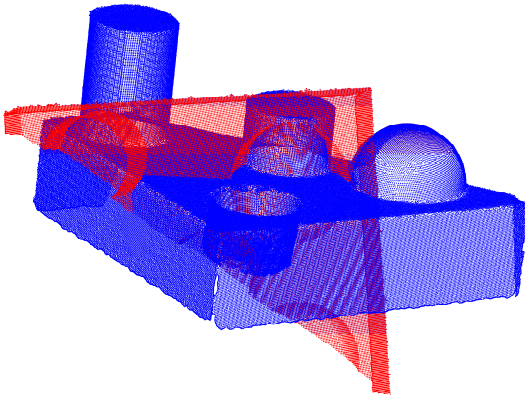

(a) Two partial scans of the plastic model.

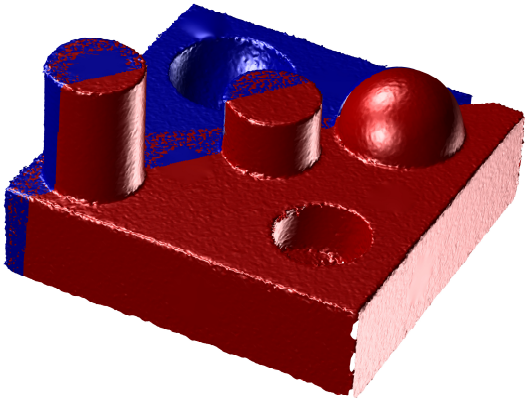

(b) Complete model created using the extracted primitives for alignment.

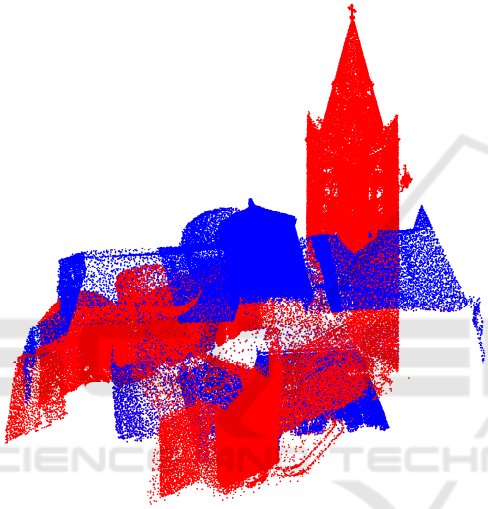

(c) Two partial point clouds of the church in the town of LansleVillard (France). The church is scanned with a LEICA Cyrax scanner.

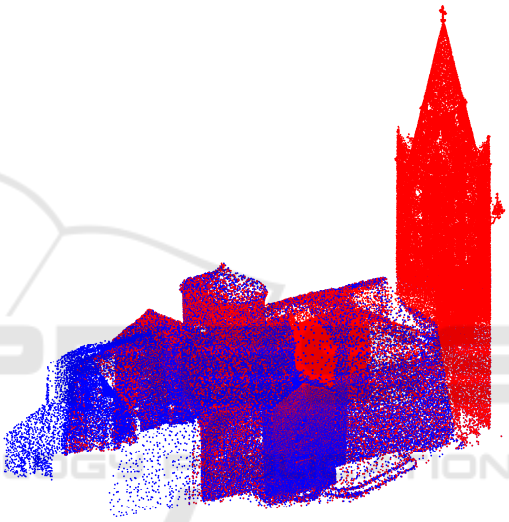

(d) The church model is built by aligning the extracted planes from partial data.

Figure 7: Complete models are created from partial data using the proposed method of primitive alignment.

4 CONCLUSION

An efficient and robust method for registering two basic primitives is proposed in this paper. Using a new optimization technique and with the addition of a complementary objective function, the convergence is guaranteed to achieve accurate results. The proposed method can benefit other applications such as scan alignment, quality control and inspection.

Currently, the framework of primitive-based registration manually assigns the correspondence pairs of primitives between datasets. An automatic detection of the correspondence between primitives will be the object of future work.

ACKNOWLEDGEMENT

This research project was supported by the NSERC/Creaform Industrial Research Chair on 3-D Scanning. The authors thank to AIM@SHAPE for providing the scanned data of the church in Fig. 7. We are grateful to Annette Schwerdtfeger for proofreading the manuscript.

REFERENCES

Attene, M., Falcidieno, B., and Spagnuolo, M. (2006). Hierarchical mesh segmentation based on fitting primitives. *The Visual Computer*, 22(3):181–193.

Besl, P. and McKay, N. D. (1992). A method for registration of 3-D shapes. *IEEE Transactions on Pattern Analysis and Machine Intelligence*, 14(2):239–256.

Bosché, F. (2012). Plane-based registration of construction laser scans with 3D/4D building models. *Advanced Engineering Informatics*, 26(1):90–102.

Chao, C. and Stamos, I. (2005). Semi-automatic range to range registration: a feature-based method. In *Proceedings of the Fifth International Conference on 3-D Digital Imaging and Modeling*, pages 254–261. IEEE.

Díez, Y., Roure, F., Lladó, X., and Salvi, J. (2015). A qualitative review on 3D coarse registration methods. *ACM Computing Surveys*, 47(3):45.

Forsgren, A., Gill, P. E., and Wright, M. H. (2002). Interior methods for nonlinear optimization. *SIAM review*, 44(4):525–597.

Horn, B. K. (1987). Closed-form solution of absolute orientation using unit quaternions. *Journal of the Optical Society of America A*, 4(4):629–642.

Marquardt, D. W. (1963). An algorithm for least-squares estimation of nonlinear parameters. *Journal of the Society for Industrial & Applied Mathematics*, 11(2):431–441.

Planitz, B. M., Maeder, A. J., and Williams, J. (2005). The correspondence framework for 3D surface matching algorithms. *Computer Vision and Image Understanding*, 97(3):347–383.

Press, W. H., Teukolsky, S. A., Vetterling, W. T., and Flannery, B. P. (2007). *Numerical Recipes 3rd Edition: The Art of Scientific Computing*. Cambridge University Press, New York, NY, USA, 3 edition.

Rabbani, T., Dijkman, S., van den Heuvel, F., and Vosselman, G. (2007). An integrated approach for modelling and global registration of point clouds. {*ISPRS*} *Journal of Photogrammetry and Remote Sensing*, 61(6):355 – 370.

Rusinkiewicz, S. and Levoy, M. (2001). Efficient variants of the ICP algorithm. In *Proceedings Third International Conference on 3-D Digital Imaging and Modeling*, pages 145–152. IEEE.

Salvi, J., Matabosch, C., Fofi, D., and Forest, J. (2007). A review of recent range image registration methods with accuracy evaluation. *Image and Vision Computing*, 25(5):578–596.

Stamos, I., Liu, L., Chen, C., Wolberg, G., Yu, G., and Zokai, S. (2008). Integrating automated range registration with multiview geometry for the photorealistic modeling of large-scale scenes. *International Journal of Computer Vision*, 78(2-3):237–260.

Tam, G. K., Cheng, Z.-Q., Lai, Y.-K., Langbein, F. C., Liu, Y., Marshall, D., Martin, R. R., Sun, X.-F., and Rosin, P. L. (2013). Registration of 3D point clouds and meshes: a survey from rigid to nonrigid. *IEEE Transactions on Visualization and Computer Graphics*, 19(7):1199–1217.

Tombari, F., Salti, S., and Di Stefano, L. (2013). Performance evaluation of 3D keypoint detectors. *International Journal of Computer Vision*, 102(1-3):198–220.

Tran, T.-T., Cao, V.-T., and Laurendeau, D. (2015a). Extraction of cylinders and estimation of their parameters from point clouds. *Computers & Graphics*, 46:345 – 357.

Tran, T.-T., Cao, V.-T., and Laurendeau, D. (2015b). Extraction of reliable primitives from unorganized point clouds. *3D Research*, 6(4).

Tran, T.-T., Cao, V.-T., and Laurendeau, D. (2016). esphere: extracting spheres from unorganized point clouds. *The Visual Computer*, pages 1–18.